We are IntechOpen,
the world's leading publisher of Open Access books
Built by scientists, for scientists

4,800
Open access books available

122,000
International authors and editors

135M
Downloads

Our authors are among the

154
Countries delivered to

TOP 1%
most cited scientists

12.2%
Contributors from top 500 universities

BOOK CITATION INDEX — CLARIVATE ANALYTICS — INDEXED

WEB OF SCIENCE™

Selection of our books indexed in the Book Citation Index
in Web of Science™ Core Collection (BKCI)

Interested in publishing with us?
Contact book.department@intechopen.com

Numbers displayed above are based on latest data collected.
For more information visit www.intechopen.com

Statistical Analysis of Wind Tunnel and Atmospheric Boundary Layer Turbulent Flows

Adrián Roberto Wittwer,
Guilherme Sausen Welter and Acir M. Loredo-Souza

Additional information is available at the end of the chapter

1. Introduction

Many studies on wind engineering require the use of different types of statistical analysis associated to the phenomenology of boundary layer flows. Reduced Scale Models (RSM) obtained in laboratory, for example, attempt to reproduce real atmosphere phenomena like wind loads on buildings and bridges and the transportation of gases and airborne particulates by the mean flow and turbulent mixing. Therefore, the quality of the RSM depends on the proper selection of statistical parameters and in the similarity between the laboratory generated flow and the atmospheric flow.

The turbulence spectrum is the main physical parameter used to compare the velocity fluctuation characteristics of atmospheric and laboratory flows in Wind Load Modeling (WLM). This is accomplished by fitting experimental spectra to some functional form, *e.g.*, von Kármán, Harris or Batchelor-Kaimal formula, and then creating dimensionless turbulence spectra in accordance with a similarity theory [1, 2, 3]. The objective behind the use of a similarity theory is that the dimensionless spectra of atmospheric and laboratory flows collapse, if the dimensionless spectra were constructed by appropriate parameters [4].

This classical spectral comparison is commonly used in WLM [5]. However, some difficulties, related to the determination of the inertial range extent, choice of characteristic velocity and length scale parameters and possible effects due to the finiteness of the Reynolds number arise in wind tunnel studies, specially, when simulations are performed at low velocities [6].

Considering this scenario, a complementary study taking into account the use of local scale based Reynolds number, inertial and dissipation range characteristic scales, control of sampling frequency and post-processing filtering is proposed. Selected data sets obtained under

distinct configurations of three wind tunnels, a smooth pipe and atmospheric boundary layer are used. In addition, a different class of spectral representation proposed by Gagne et al. [7], which is based on local similarities and compatible with the multifractal formalism, is compared to traditional approaches.

2. Atmospheric boundary layer flows and wind tunnel flow simulation

The atmospheric boundary layer is the lowest part of atmosphere. Effects of the surface roughness, temperature and others properties are transmitted by turbulent movement in this layer. Under conditions of weak winds and very stable stratification, turbulent exchanges are very weak and the atmospheric boundary layer is called surface inversion layer [8]. A distinction is usually made between atmospheric boundary layer over homogeneous and non-homogeneous terrain. In this last situation, the boundary layer is not well defined, and topographical features could cause highly complex flows.

The depth of the atmospheric boundary layer varies with the atmospheric condition, but it is typically 100 m during the night-time stable conditions and 1 km in daytime unstable or convective conditions. A detailed description related to the wind characteristics associated to the neutral condition is made by Blessmann [3] in his book on Wind in Structural Engineering. Several similarity theories have been proposed for different atmospheric stability conditions. Near the surface, from dimensional arguments the analysis leads to the Prandtl logarithmic law, Eq. (1), in the case of a neutral boundary layer:

$$\frac{U(z)}{u^*} = \frac{1}{0.4} \ln \frac{z - z_d}{z_0} \tag{1}$$

Where U is the mean velocity, u^* is the friction velocity, z_0 is know as the roughness height and z_d is defined as the zero-plane displacement for very rough surface. The depth of a wind tunnel boundary layer is defined as the height where mean velocity reaches 0.99 of the free stream velocity. This definition is used to characterize atmospheric flow simulations.

Wind tunnels are designed to obtain different air flows, so that similarity studies can be performed, with the confidence that actual operational conditions will be reproduced. Once a wind tunnel is built, the first step is the evaluation of the flow characteristics and of the possibility of reproducing the flow characteristics for which the tunnel was designed. Many evaluation studies of wind tunnels are presented in the open literature. Some of which are the work of Cook [9] on the wind tunnel in Garston, Watford, UK, the presentation of the closed-return wind tunnel in London [10] and the Oxford wind tunnel, UK [11], the characterization of the boundary layer wind tunnel of the UFRGS, Brazil [12] and of the Danish Maritime Institute, Denmark [13].

Wind tunnel modeling of atmospheric boundary layer is generally oriented to neutrally stable flows. Modeling of stratified boundary layer is more difficult to implement and less used

in wind tunnel tests. Similarity criteria imply that a set of non-dimensional parameters should be the same in model and prototype. In general, the flow is governed by the boundary conditions and the Rossby, Reynolds, Strouhal, Froude, Eckert and Prandtl numbers, but in most of the situations of practical importance the effects of several non-dimensional numbers can be neglected. Later studies in atmospheric boundary layer simulations attempted to reproduce as closely as possible the mean velocity distribution and turbulence scales of the atmospheric flow. This is made by non-dimensional comparisons of mean and fluctuating velocity measurements in the wind tunnel flow and atmospheric data.

In general, wind tunnel evaluation is performed at the highest flow velocity, the results being presented in terms of mean velocity distributions, turbulence intensities and scales. However, many simulations are performed at low velocities to evaluate some specific problems. This is the case of laboratory simulation of dispersion problems [14] and transmission line modeling [15].

Boundary-layer simulations are performed with help of grids, vortex generators and roughness elements, to facilitate the growth of the boundary layer and to define the mean velocity profile. This is used in the most applied simulation methods, namely the full-depth simulation [16] and part-depth simulation [17]. The use of jets and grids is also applied [12].

The "Jacek Gorecki" wind tunnel, located at the Universidad Nacional del Nordeste, UNNE at Resistencia (Chaco), Argentina, is a low velocity atmospheric boundary-layer wind tunnel, built with the aim to perform aerodynamic studies of structural models. The atmospheric boundary layer is reproduced with help of surface roughness elements and vortex generators, so that natural wind simulations are performed. Fig. 1 shows a view of the "Jacek Gorecki" wind tunnel, which is a 39.56 m long channel. The air enters through a contraction, passing a honeycomb prior to reach the test section, which is a 22.8 m long rectangular channel (2.40 m width, 1.80 m height). Two rotating tables are located in the test section to place structural models. Conditions of zero pressure gradient boundary layers can be obtained by vertical displacement of the upper wall. The test section is connected to the velocity regulator and to the blower, which has a 2.25 m diameter and is driven by a 92 kW electric motor at 720 rpm. A diffuser decelerates the air before leaving the wind tunnel.

In this wind tunnel, many models of atmospheric boundary layer were implemented. In general, the simulation of natural wind on the atmospheric boundary layer was performed by means of the Counihan and Standen methods [18, 19, 20]. To illustrate this type of flow model, an example of full-depth Counihan simulation with velocity distributions corresponding to a class III terrain is presented. According to Argentine Standards CIRSOC 102 [21], this type of terrain is designed as "ground covered by several closely spaced obstacles in forest, industrial or urban zone". The mean height of the obstacles is considered to be about 10 m, while the boundary layer thickness is $z_g = 420$ m. The power law for velocity distribution is given by

$$\frac{U(z)}{U(z_g)} = \left(\frac{z}{z_g}\right)^{\alpha} \tag{2}$$

with suitable values for the exponent a between 0.23 and 0.28 [3]. This law is of good application in neutral stability conditions of strong winds, typical for structural analysis. For this Counihan full-depth simulation, where the complete boundary-layer thickness is simulated, four 1.42 m (Hv) high elliptic vortex generators and a 0.23 m (b) barrier were used, together with prismatic roughness elements placed on the test section floor along 17 m (l) (see Fig. 2). The wind tunnel test section and the simulation hardware are shown in Fig. 3.
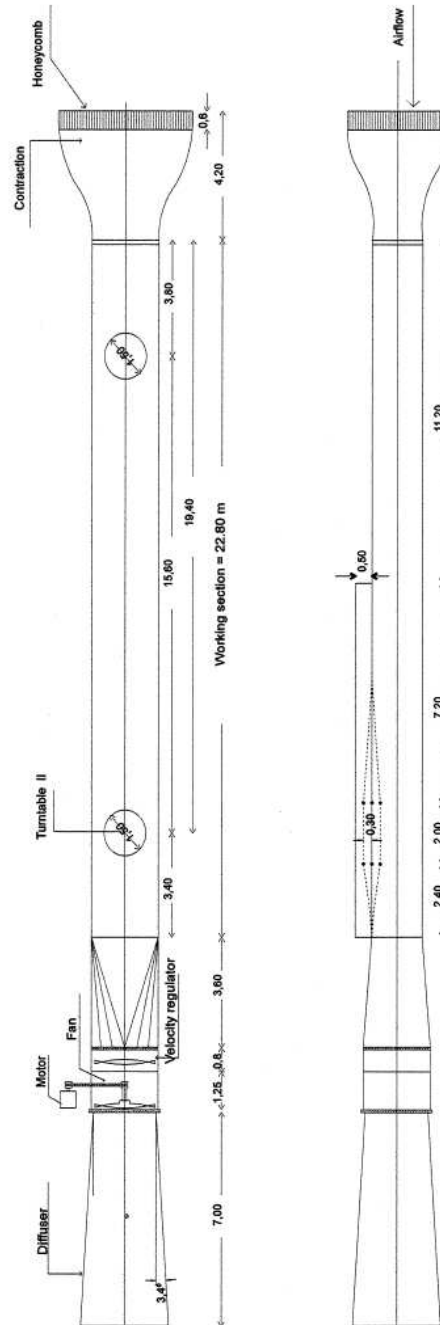

Figure 1. "Jacek Gorecki" Wind Tunnel at UNNE.

In this work, measurements of wind velocity realized in three different wind tunnels will be used for the spectral analysis. The *"Jacek Gorecki"* wind tunnel [19] described above, the *"TV2"* wind tunnel of the Laboratorio de Aerodinámica, UNNE, smaller, also an open circuit tunnel, and the closed return wind tunnel *"J. Blessmann"* of the Laboratório de Aerodinâmica das Construçoes, Universidade Federal de Rio Grande do Sul, UFRGS [12].
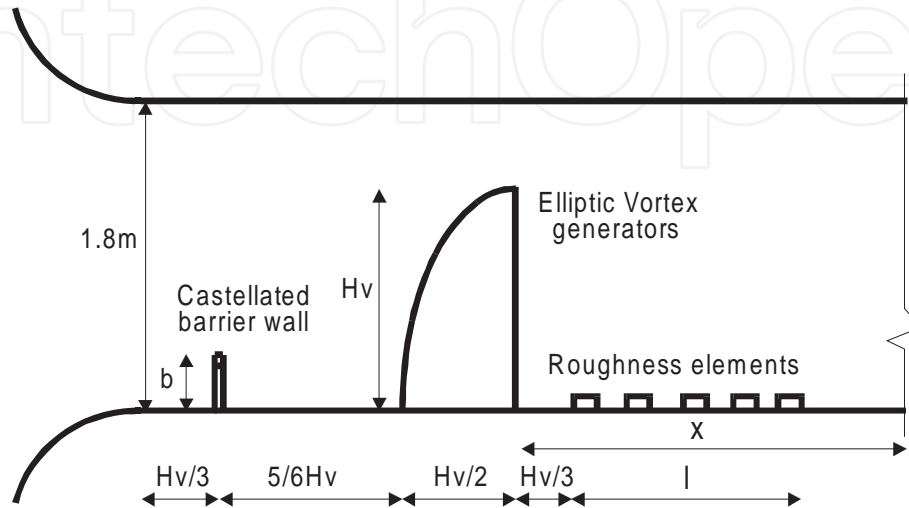

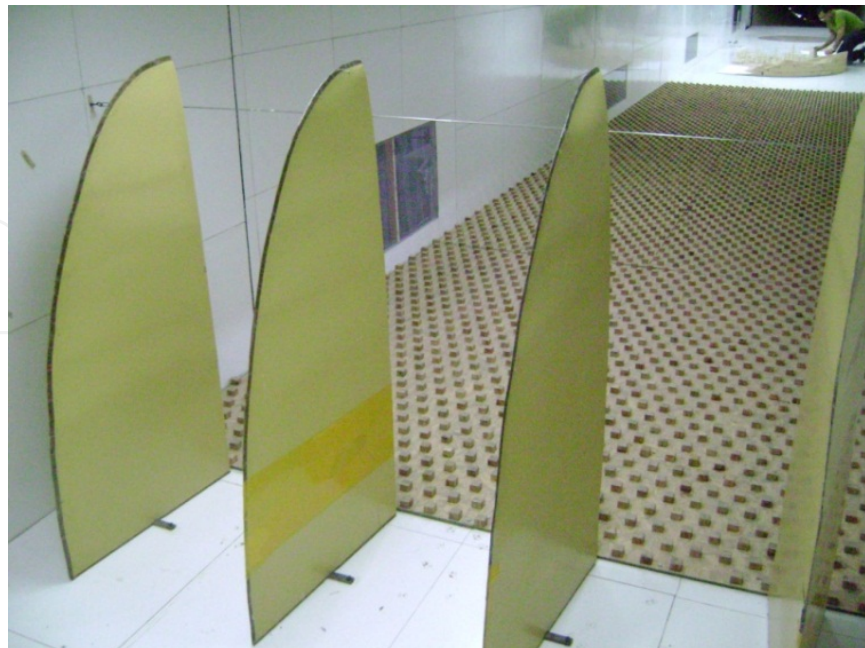**Figure 2.** Arrangement of Counihan simulation hardware.

Figure 3. Test section and full-depth Counihan vortex generators.

3. Mean flow evaluation of an atmospheric boundary layer simulation

The above described Counihan simulation is used to illustrate the mean flow evaluation. In this case, mean velocity measurements were performed by means of a pitot-Prandtl tube connected to a Betz manometer. Velocity and longitudinal velocity fluctuations were measured by a constant temperature hot wire anemometer, with a true-RMS voltmeter, using low and high-pass analogical filters. Data acquisition of hot wire signals was made by means of an A/D board connected to a personal computer. Uncertainty associated with the measured data depends of the hot wire resolution and the calibration system. In this case, an uncertainty order of ± 3 % was determined at high velocity measurements.

Previously to simulate ABL flows, an empty tunnel flow evaluation was realized. Mean velocity profiles were measured along a vertical line on the center of the rotating table 2. The boundary layer has a thickness of about 0.3 m and the velocity values have a maximal deviation of 3 %, by taking the velocity at the center of the channel as reference. Turbulence intensity distribution at the same locations shows values around 1% outside the boundary layer increasing, as expected, inside the boundary layer. Reference velocity at the center of the channel for empty tunnel tests was 27 m/s and the resulting Reynolds number 3.67×10^6.

Once the empty tunnel evaluation was over, the mean flow of the full-depth boundary layer simulation was analyzed. Measurement of the mean velocity distribution was made along a vertical line on the center of rotating table 2 and along lines 0.30 m to the right and left of this line. Fig. 4 shows the velocity distribution along the central line. Flow characteristics are presented in Table 1. There is a good similarity among the velocity profiles given by the values of the exponent α obtained. Turbulence intensity distribution at the same locations is shown in Fig. 5. The values are lower than those obtained by Cook [4] and by using Harris-Davenport formula for atmospheric boundary layer [3]. Values are reduced as the distance from the lower wall is increased.
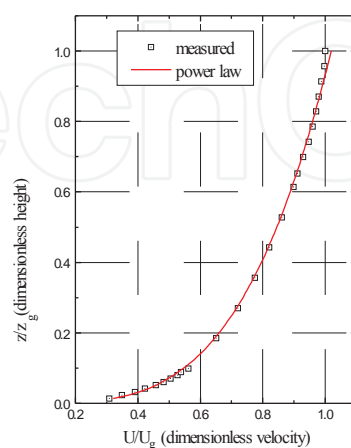

Figure 4. Vertical mean velocity profile – experimental values and power law fit.

These mean velocity and turbulence intensity vertical profiles show a typical evaluation of the boundary layer mean flow applied to wind load studies. Similar analysis was made for other authors to different wind tunnel simulations. Some works include vertical profiles of longitudinal turbulence scales [12, 20]. When dispersion problems are analyzed and physic atmospheric research studies in wind tunnel are development the mean flow evaluation is usually realized utilizing the logarithmic expression, Eq. (1). A simple method to fit experimental values of mean velocity to the logarithmic law is presented by Liu et al. [22]. The characteristic parameters u^* and z_0, friction velocity and roughness height, respectively, are used to evaluate critical Reynolds number values on low velocity tests for wind tunnel dispersion studies [23].

	$y = 0$	$y = 0.30$ m	$y = -0.30$ m
z_g[m]	1.164	1.164	1.164
U_g[m/s]	27.51	28.18	27.76
α	0.270	0.265	0.270

Table 1. Flow characteristics for full-depth boundary layer simulation.
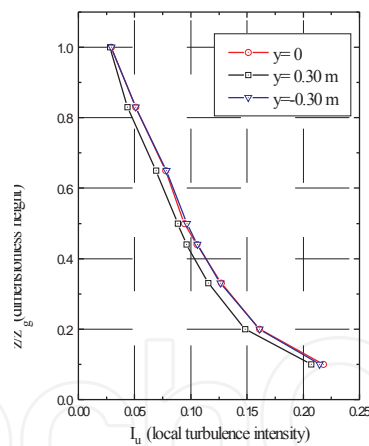

Figure 5. Vertical turbulence intensities profiles.

4. Energy spectra and structure functions in boundary layer flows

Atmospheric data come from anemometers frequently located 10 m height. These values contain climatic system contributions and components of the boundary layer itself. That is, measured data include wind velocity variations corresponding to time scales from some

hours to fractions of one second. Usually power spectra are employed to analyze these atmospheric records. The Van der Hoven spectrum, obtained in Brookhaven, Long Island, NY, USA [24], represents the energy of the longitudinal velocity fluctuation on the complete frequency domain. Two peaks can be distinguished in this spectrum, one corresponding to the 4-day period or 0.01 cycles/hour (macro-meteorological peak), and another peak between the periods of 10 minutes and 3 seconds associated to the boundary layer turbulence (micro-meteorological peak). A spectral valley, with fluctuations of low energy, is observed between the macro and micro-meteorological peak. This region is centered on the period of 30 minutes and allows dividing the mean flow and the velocity fluctuations. This spectral characteristic confirms that interaction between climate and boundary layer turbulence is negligible and permits considering both aspects independently.

Velocity fluctuations with periods lower than one hour define the micro-meteorological spectral region or the atmospheric turbulence spectrum. Interest of wind load and dispersion problems is concentrated on this spectral turbulence region. In 1948 von Kármán suggested an expression for the turbulence spectrum with which his name is related, and 20 years later this spectral formula started to be used for wind engineering applications. Some deficiencies in fitting data measured in atmospheric boundary layer were pointed later and Harris [5] shown a modified formulae for the von Kármán spectrum.

According ESDU [3], the von Kármán formula for the dimensionless spectrum of the longitudinal component of atmospheric turbulence is:

$$\frac{fS_u}{\sigma_u^2} = \frac{4X_u(z)}{\left[1 + 70{,}78X_u(z)^2\right]^{5/6}} \tag{3}$$

where S_u is the spectral density function of the longitudinal component, f is the frequency in Hertz and σ_u^2 is the variance of the longitudinal velocity fluctuations. The dimensionless frequency $X_u(z)$ is $fL(z)/U(z)$, being L the integral scale. This spectrum formula satisfies the Wiener-Khintchine relations between power spectra and auto-correlations and provides a Kolmogorov equilibrium range in the spectrum. However, the von Kármán expression provides no possibility to fit other measured spectral characteristics [5].

Two situations of spectral analysis of boundary layer flow are presented next from different wind tunnel studies and atmospheric data. These cases resume a typical spectral evaluation of a boundary layer simulation and a spectral comparison of different boundary layer flows. Finally, a discussion of the use of structure functions applied to the analysis of velocity fluctuations is presented.

4.1. Spectral evaluation of a wind tunnel boundary layer simulation

A first example of spectral analysis is that corresponding to the Counihan boundary layer simulation described on previous section. Longitudinal velocity fluctuations were measured by the hot wire anemometer system and the uncertainty associated with the measured data is the same as previously mentioned. In this case, spectral results from longitudinal velocity

fluctuations were obtained by juxtaposing three different spectra from three different sampling series, obtained in the same location, each with a sampling frequency, as given in Table 1, as low, mean and high frequencies. The series were divided in blocks to which an FFT algorithm was applied [25]. In Fig. 6, four spectra obtained at height z=0.233, 0.384, 0.582 and 0.966 m are shown. Values of the spectral function decrease as the distance from the tunnel floor z is increased. An important characteristic of the spectra is the presence of a clear region with a -5/3 slope, characterizing Kolmogorov's inertial sub-range.

The comparison of the results obtained through the simulations with the atmospheric boundary layer is made by means of dimensionless variables of the auto-spectral density fS_u/σ_u^2 and of the frequency $X_u(z)$ using the von Kármán spectrum, given by the expression of Eq. (3). Kolmogorov's spectrum will have, therefore, a -2/3 exponent instead of -5/3. The comparison was realized for spectra measured at different heights, but only is presented the spectrum obtained at $z = 0.233$ m (Fig. 7). The agreement is very good, except for the highest frequencies affected by the action of the low-pass filter.

	Low frequency	Mean frequency	High frequency
Sampling frequency [Hz]	300	900	3000
Low-pass filter [Hz]	100	300	1000
High-pass filter [Hz]	0.3	0.3	0.3
Sampling time [s]	106.7	35.6	10.7
Bandwidth [Hz]	1.132	3.516	11.719

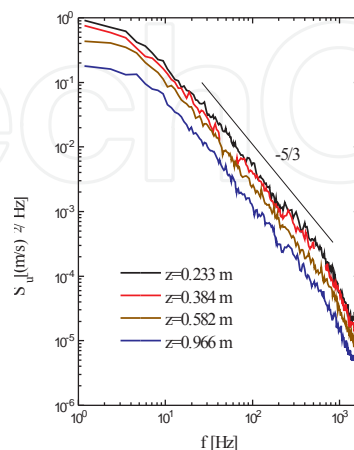**Table 2.** Data acquisition conditions for spectral analysis.

Figure 6. Power spectra of the longitudinal velocity fluctuation for a boundary layer simulation.

This evaluation was realized at high velocity ($U_g \approx 27$ m/s) being the resulting Reynolds number value of Re $\approx 4\times10^6$. The juxtaposing technique used to improve the spectral resolution is today unnecessary because of the fact that is possible to utilize a large sample size. However, sample series were limited to 32000 values for this analysis and three spectra were juxtaposed.

A scale factor of 250 for this boundary layer simulation was obtained through the procedure proposed by Cook [4], by means of the roughness length z_0 and the integral scale L_u as parameters. The values of the roughness length are obtained by fitting experimental values of velocity to the logarithmic law of the wall, while integral scale is given by fitting the values of the measured spectrum to the design spectrum.
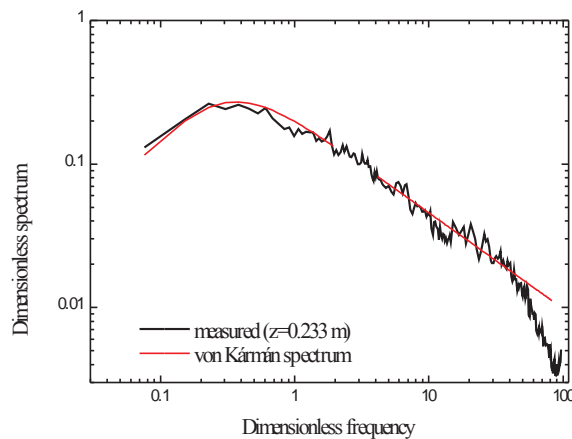

Figure 7. Comparison of the dimensionless spectrum obtained at z = 0.233 m and the von Kármán spectrum.

4.2. Spectral comparison of different boundary layer flows

A second study based on results of different boundary layer flows was realized. Measurements of the longitudinal fluctuating velocity obtained in three different wind tunnels were selected for this analysis. All selected velocity samples correspond to neutral boundary layer flow simulations developed in appropriate wind tunnels. The analysis was complemented using measurements realized in a smooth tube flow and in the atmosphere.

Wind tunnel and smooth tube measurements were realized by a constant hot-wire anemometer previously described. Atmospheric data were obtained using a Campbell 3D sonic anemometer [26], for which the resolution is 0.01 m/s for velocity measurements. Table 3 indicates a list of sampling characteristics, being z the vertical position (height), U the mean velocity, σ_u^2 the variance of fluctuations velocity, f_{acq} the acquisition frequency, L_u the integral scale and Re_L the Reynolds number associated to L_u.

One of the three wind tunnels used to obtain the wind data employed in this experimental analysis is the *"Jacek Gorecki"* wind tunnel described on a previous section. The second is the

"*TV2*" wind tunnel of the Laboratorio de Aerodinámica, UNNE, too. The "*TV2*", smaller, is also an open circuit tunnel with dimensions of 4.45×0.48×0.48m (length, height, width). The study was complemented by the analysis of measurements realized on atmospheric boundary layer simulations performed in the closed return wind tunnel "Joaquim Blessmann" of the Laboratório de Aerodinâmica das Construçoes, Universidade Federal de Rio Grande do Sul, UFRGS [12]. The simulations of natural wind on the atmospheric boundary layer were performed by means of the Counihan [16] and Standen [17] methods, with velocity distributions corresponding to a forest, industrial or urban terrain. The tube measurement was obtained in the centre of a 60 mm diameter smooth tube. Atmospheric data were obtained in a micrometeorological station located at Paraiso do Sul, RS, Brasil [26, 27].

	z [m]	U [m/s]	σ_u^2 [m²/s²]	f_{acq}[Hz]	L_u [m]	Re_L
Smooth tube	0.03	38.89	1.63	16	0.034	8.83×10^4
Atmosphere	10.00	4.51	3.32	16	36.30	1.09×10^7
Blessman WT-LV	0.15	3.18	0.19	1024	0.51	1.08×10^5
Gorecki WT-LV	0.21	2.97	0.26	1024	0.26	5.16×10^4
Gorecki WT-HV[(+)]	0.21	16.77	7.55	2048	0.51	5.71×10^5
TV2 WT-LV	0.04	0.68	0.03	900	0.07	3.18×10^3
TV2 WT-HV	0.04	11.69	4.92	3000	0.11	8.59×10^4

Table 3. Measurement characteristics for spectral analysis.

The measurements realized in the J. Gorecki wind tunnel at high velocity were used to analyze the sampling effects on the spectral characteristics. Five different samplings were realized for measurements Gorecki WT-HV[(+)] at z= 0.21 m. Sampling characteristics like frequency acquisition f_{acq}, low pass frequency f_{lp} and sampling time t_s are indicated in Table 4. Resulting superposed spectra are shown in Fig. 8 where it is possible to see a good definition of the inertial sub-range (-5/3 slope) and the effect of the low pass filter.

Samples	*Sp1*	*Sp2*	*Sp3*	*Sp4*	*Sp5*
f_{acq}[Hz]	4096	2048	1024	8192	16348
f_{lp}[Hz]	3000	1000	300	3000	10000
t_s[s]	30	60	120	15	7.5

Table 4. Measurement characteristics for analysis of sampling effects.

Fig. 9 shown spectral density functions S_u corresponding to measurements indicated in Table 3. High frequencies in the atmosphere spectrum correspond to low frequencies in the smooth pipe. The same spectra in dimensionless form are presented in Figs. 10 and 11. The

frequency is non dimensionalised by fL_u/U in Fig. 10 and by fz/U in Fig. 11, according to parameters usually employed in wind engineering. In general, preliminary results permit verifying the good behavior of the wind tunnel spectra and a good definition of the inertial range (slope -5/3). The inertial sub-region is narrower for low velocity measurements (LV).

Spectral special features in smooth tube and atmosphere appear in Fig. 9 and in the dimensionless comparison too (Figs. 10 and 11). This particular behavior is a product of the uniform flow in the centre of the smooth tube, that is, not a boundary layer flow is being analyzed. In the atmospheric flow case, this type of behavior is possibly due to the existence of a convective turbulence component at low frequencies because of that atmospheric stability is not totally neutral. This behavior was verified in the case of measurements realized in near-neutral atmosphere. The existence of a low frequency convective component was detected in three dimensional measurements obtained at the atmosphere [28]. The aliasing effect is perceived at high frequencies due to high pass filter is not used for sample acquisition of atmospheric data.
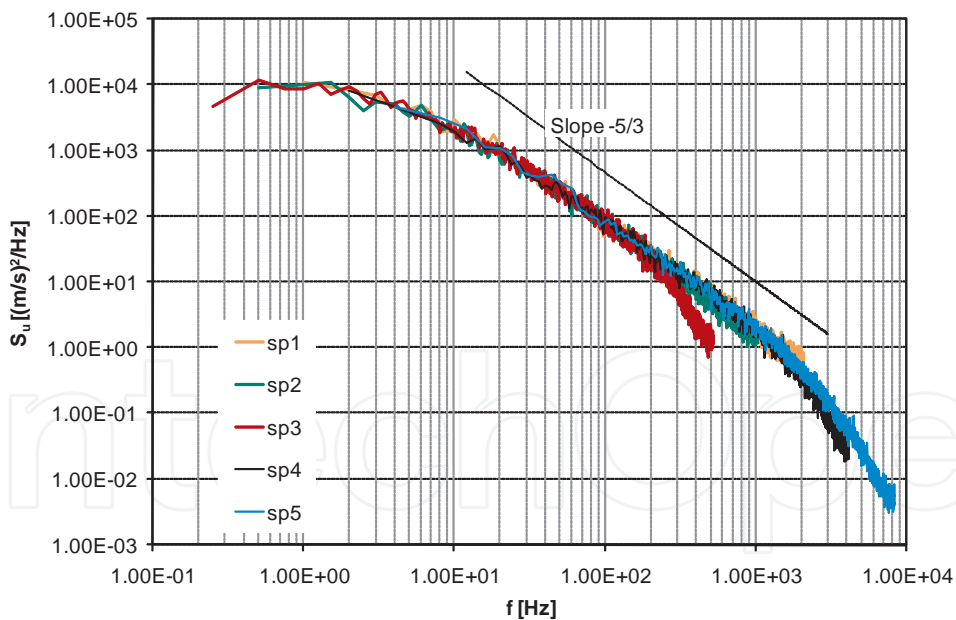

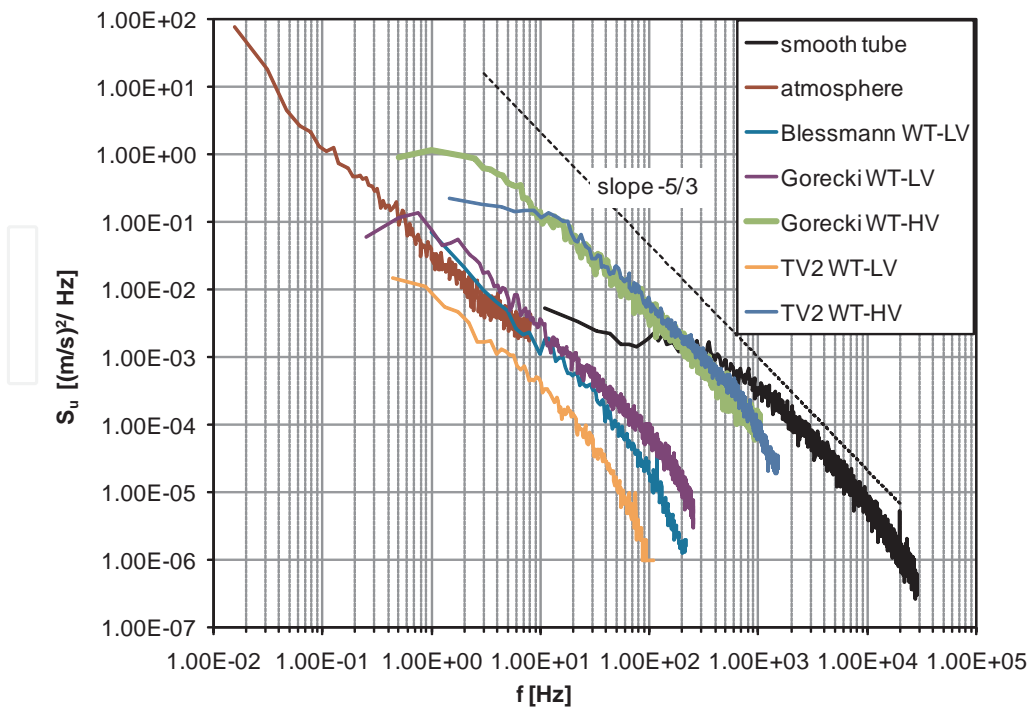**Figure 8.** Spectral superposition for different sampling.

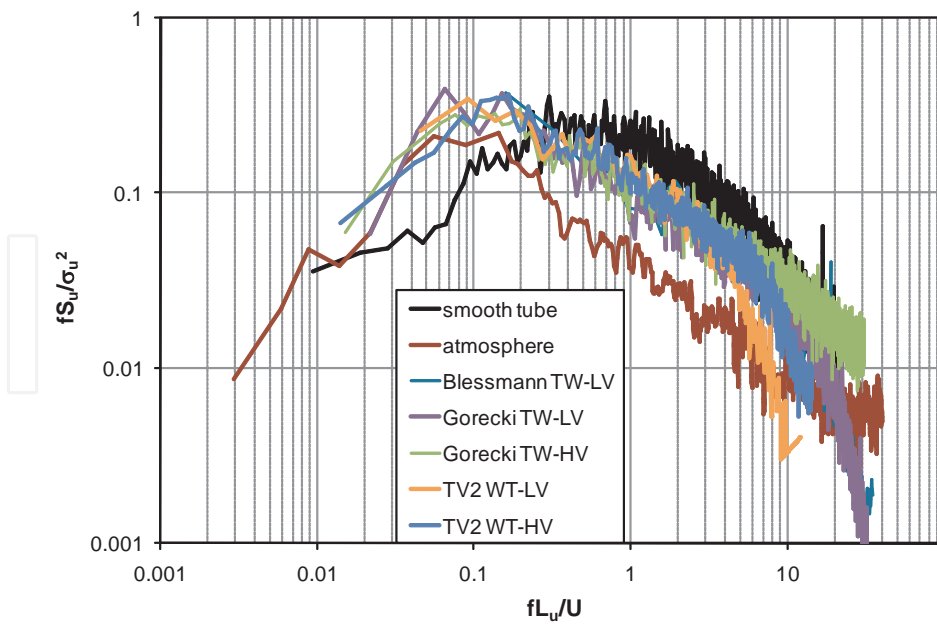**Figure 9.** Power spectra for measurements indicated on Table 3.

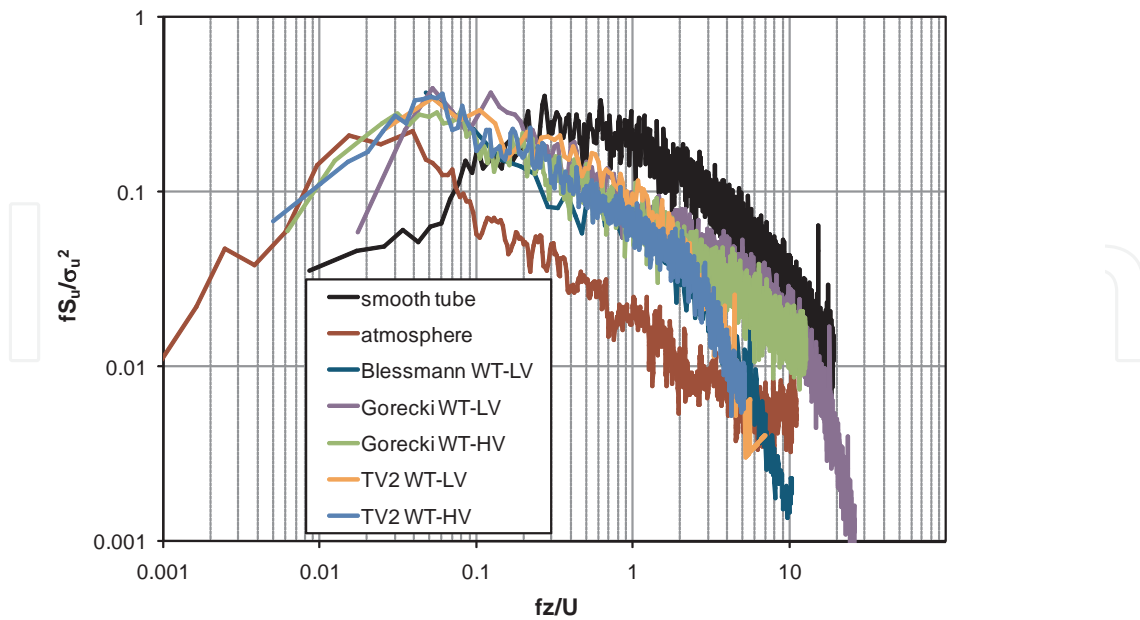**Figure 10.** Comparison of dimensionless spectra using fL_u/U.

Figure 11. Comparison of dimensionless spectra using *fz/U.*

The superposition technique allows defining precisely the sub-inertial range and extending the frequency analysis interval. Besides, it is possible defining adequately the sampling characteristics and optimizing the measuring time. In general, the spectral comparison realized using fL_u/U (Fig. 10) indicates better coincidence [27, 28]. However, the analysis realized up to now is preliminary and it should be studied in depth. For example, the methods for the parameter L_u calculation should be analyzed, the application of other parameters to obtain the dimensionless frequency at smaller scales and other measurements must be analyzed looking for the improvement of the scale modeling.

A different approach to analyze velocity fluctuations will be presented below. This is based on the high order moments of velocity increments. Small scales to characterize the boundary layer flows will be used and a new representation of energy spectra will be evaluated.

4.3. Statistical moments of velocity fluctuations

Previous type of spectral analysis is usually employed in Wind engineering. The following study is realized using velocity structure functions of turbulent boundary layer flow. These statistical moments are utilized by atmospheric physical researchers. The approach considers scales smaller than the integral scale L_u and, therefore is presumably more suitable for applications to turbulent diffusion studies. Apart from integral scales, the mean dissipation rate, the Kolmogorov and Taylor micro-scales could be obtained. On other hand, results from this type of study can be employed to analyze the Kolmogorov constant and, indirectly, for application to pollution dispersion models [30, 31].

Kolmogorov`s laws for locally isotropic turbulence [32, 33] were originally derived for structure functions from the von Kármán-Howarth-Kolmogorov equation [34],

$$S_3(r) = -\frac{4}{5}\varepsilon r + 6v\frac{d}{dr}S_2(r) \tag{4}$$

valid for $r \ll L_u$ in the limit of very large Reynolds number, where $S_p(r) = \langle [u(x+r) - u(x)]^p \rangle$ is the structure function of order p, v is the kinematic viscosity, ε is the mean dissipation rate, and $\langle \cdot \rangle$ represents statistical expectation operator.

Kolmogorov deduced the following relations for second and third-order structure functions:

$$S_2(r) = C(\varepsilon r)^{2/3} \tag{5}$$

$$S_3(r) = -\frac{4}{5}\varepsilon r, \tag{6}$$

valid for $\eta \ll r \ll L_u$, where $\eta = (v^3/\varepsilon)^{1/4}$ is the Kolmogorov microscale, and C≈2 is the Kolmogorov constant [29, 34].

The third-order structure function Eq.(6), also known as the four-fifths law, is straightforwardly obtained from Eq.(4) since, for very large Reynolds number, the second term in the right hand side of Eq.(4) can be neglected. The four-fifths law is of special interest in the statistical theory of turbulence because, besides being an exact relation, it allows a direct identification of the mean dissipation energy per unit mass with the mean energy transfer across scales [35].

The two-thirds law Eq. (3), on the other hand, is not an exact relation; it was obtained using dimensional arguments and introducing a nondimensional constant that should be empirically determined. The second-order structure function provides information about the energy content in all scales smaller than r. Moreover, the famous Kolmogorov energy spectrum $E(k) = C_k \varepsilon^{2/3} k^{-5/3}$ is derived from Eq. (5).

Table 5 shows the results of the analysis for four experiments selected from the analysis described in section 4.2. The distinct columns report the mean wind speed U, height z, inertial range (r_a, r_b), integral scale L_u, mean dissipation rate ε, Kolmogorov microscale η, Taylor's microscale based Reynolds number Re_λ. The mean dissipation rate, ε, was determined by the best fit of $S_3(r)$, Eq. (2), in the inertial range. The Kolmogorov microscale was computed by $\eta = (v^3/\varepsilon)^{1/4}$ and Taylor's microscale based Reynolds number $Re_\lambda = \sigma_u \lambda / v$ was computed from $\lambda = [\sigma_u^2 / \langle (\partial_x u)^2 \rangle]^{1/2}$, where $\langle (\partial_x u)^2 \rangle$ was indirectly estimated with the aid of the isotropic relation $\varepsilon = 15v\langle (\partial_x u)^2 \rangle$.

	z [m]	U [m/s]	(r_a, r_b)[cm]	L_u [m]	ε [m²/s³]	η [mm]	Re_λ
Smooth tube	0.03	38.89	0.35-1.10	0.034	52.9	0.08	174
Atmosphere	10.00	4.51	30-600	36.30	0.045	0.51	13141
Gorecki WT-HV	0.21	16.77	2.0-9.0	0.39	33.0	0.10	1311
TV2 WT-HV	0.04	11.69	0.3-2.0	0.13	48.8	0.09	629

Table 5. Main turbulence characteristics from laboratory and atmospheric turbulence data.

Experimental evaluations of second and third-order structure functions for the J. Gorecki wind tunnel are shown in Fig. 12. In the K41 picture, the estimation of the second-order structure function constant is reduced to an estimation of the skewness $S = S_3(r)/(S_2(r))^{3/2}$; however, differently from $S_2(r)$, $S_3(r)$ displays some noise (Fig. 12). This behavior is observed in all datasets.

One immediate consequence of the similarity arguments assumed in K41 is that graphical representation of distinct turbulence spectra should collapse in a single-curve after a proper normalization with characteristic velocity and length scales. Another consequence, which follows from dimensional analysis, is the scaling $S_p(r) \approx r^{p/3}$ for a structure function of order p, with $\eta \ll r \ll L_u$. However, inertial range physics has been proved to be much more complex than previously assumed in the K41. A remarkable consequence of this complexity, which has close relation with the small scale intermittency phenomenon [33], is the existence of anomalous scaling concerning structure functions exponents, $S_p(r) \approx r^{\zeta_p}$, where ζ_p is non linear function of p. The multifractal formalism was then introduced by Parisi and Frisch in order to provide a robust framework, allowing the analysis and interpretation for a general class of complex phenomena presenting anomalous scaling.

One important difference between the multifractal interpretation of turbulence and the (monofractal) K41 theory is the assumption of a local similarity scaling for small scales. The global scaling similarity assumed in the K41 theory is still at the core of the most wind tunnel and atmospheric turbulence modeling [5, 28, 34]. The local scaling similarity ideas of the multifractal formalism, on the other side, provide a new vocabulary, enabling interpretation and comparison of diverse multiscale phenomena. Although the multifractal formalism has been used in many areas of applied physics, does not share the same popularity in the fields of engineering.

According to the multifractal universality [36], a single-curve collapse of distinct experimental turbulence spectra is obtained by plotting $\log E(k)/\log Re$ against $\log k/\log Re$, after having properly normalized $E(k)$ and k. On the other hand, an alternative similarity plot has been proposed by Gagne et al. [7] based on an intermittency model, but still compatible with the multifractal formalism. These authors propose that a better merging of experimental

spectra can be obtaining by plotting $\beta \log \left(a E(k)(\varepsilon \nu^5)^{-1/4} \right)$ against $\beta \log \left(c k (\nu^3/\varepsilon)^{1/4} \right)$, with $\beta = 1/\log(\mathrm{Re}_\lambda / R^*)$, where Re_λ is the Taylor scale based Reynolds number and the empirical constants $R^* = 75$, $a = 0.154$, and $c = 5.42$ were determined to provide the best possible super-position in their dataset.

In Fig. 13 the plot proposed by Gagne et al. [7] is presented for laboratory and atmospheric turbulence data. Despite the fact that data comprise very different scales, $L_u \approx 10^2$ m for at-mospheric data, and $L_u \approx 10^{-1}$ m for smooth pipe, the merging of spectra is reasonably good, also regarding the fact that the originally proposed empirical constants have been used in the present dataset.

In this representation the slopes remain unchanged, but the extent of inertial range presum-ably has the same length for all spectra. Although a solid ground for the physics behind the representation is lacking, it is clear that the properties provided by such a representation can be very useful for physical analysis and modeling of turbulence.
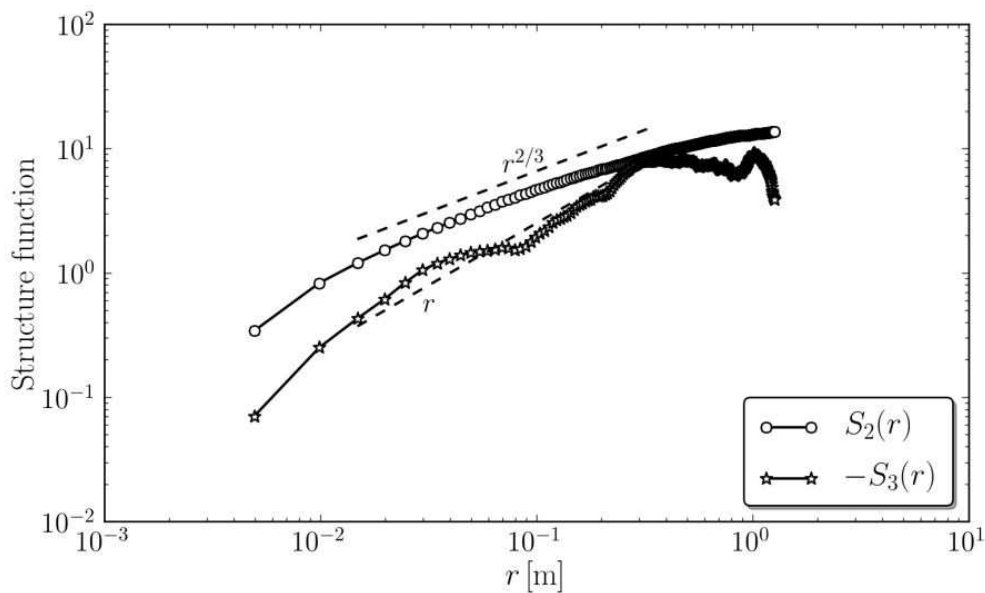

Figure 12. Second and third-order structure functions for the Gorecki WT measurement.
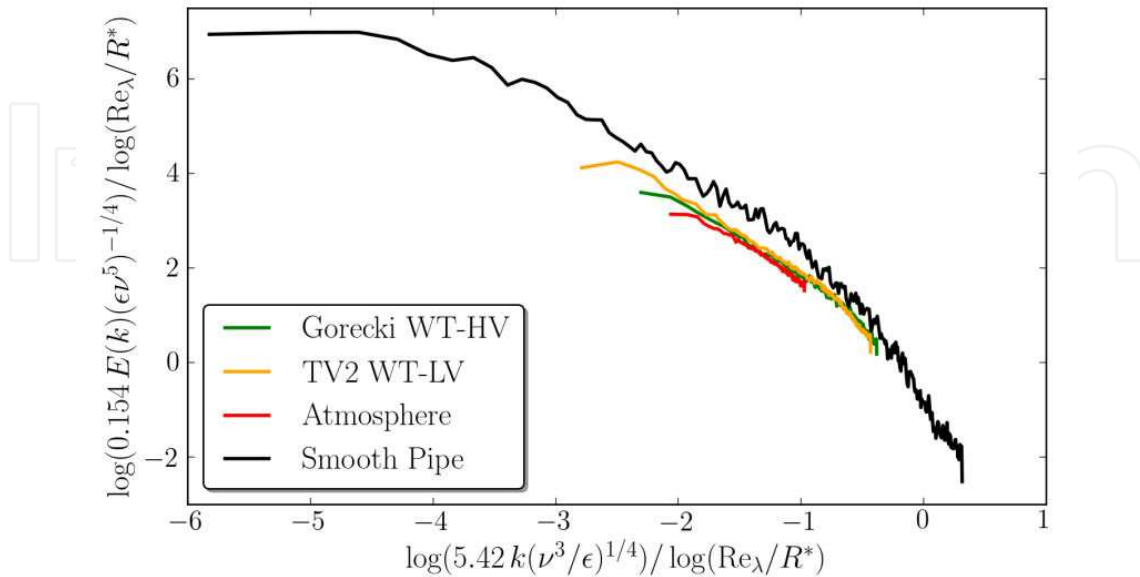
Figure 13. Single-curve spectral collapse from laboratory and atmospheric turbulence data (Table 5), as proposed by Gagne et al. [7].

5. Concluding remarks

Fully developed turbulence measurements from the laboratory and the atmospheric boundary layer encompassing a wide range of Reynolds number were analyzed in this study. First, a typical spectral evaluation of a boundary layer simulation was presented. The spectral agreement is very good and the wind simulation can be considered adequate for wind load modeling.

Next, a spectral dimensionless comparison of different boundary layer flows was realized by usual parameters in wind engineering. Measurements of the longitudinal fluctuating velocity obtained in different wind tunnels, a smooth tube and the atmosphere were selected. An analysis of sampling effects was realized and some limitations on this classical spectral comparison were established.

Finally, a discussion of the use of structure functions to investigate turbulent boundary layer flows was proposed. Turbulent scales smaller than the integral scale were determined and the behavior of second and third-order structure functions were analyzed. A single-curve collapse of distinct experimental spectra was obtained. This type of analysis should be applied to verify boundary layer flows at low speed used for dispersion modeling. Time scales for fluctuating process modeling could be improved too by applying this analysis method.

Acknowledgements

Author details

Adrián Roberto Wittwer[1], Guilherme Sausen Welter[2] and Acir M. Loredo-Souza[3]

*Address all correspondence to: a_wittwer@yahoo.es

1 Facultad de Ingeniería, Universidad Nacional del Nordeste, Argentina

2 Laboratório Nacional de Computação Científica, Brasil

3 Universidade Federal de Rio Grande do Sul, Brasil

References

[1] Kaimal, J. C., Wyngaard, J. C., Izumi, Y., Cote, O. R., "Spectral characteristics of surface-layer turbulence", Quart. J. R. Met. Soc. 1972, 98: 563-589.

[2] Kaimal, J. C., "Atmospheric boundary layer flows: their structure and measurement", Oxford University Press, Inc., New York, 1994.

[3] Blessmann, J., "O Vento na Engenharia Estrutural", Editora da Universidade, UFGRS, Porto Alegre, Brasil, 1995.

[4] Cook, N. J., Determination of the Model Scale Factor in Wind-Tunnel Simulations of the Adiabatic Atmospheric Boundary Layer, Journal of Industrial Aerodynamics, 1978, 2: 311-321.

[5] Harris, R. I., "Some further thoughts on the spectrum of gustiness in strong winds", J. of Wind Eng. & Ind. Aerodyn. 1990, 33: 461-477.

[6] Isymov, N., Tanaka, H., "Wind tunnel modelling of stack gas dispersion – Difficulties and aproximations", Wind Engineering, Proceedings of the fifth International Conference, Fort Collins, Colorado, USA, 1980, Ed. by J. E. Cermak, Pergamon Press Ltd.

[7] Y. Gagne, M. Marchand and B. Castaing, A new representation of energy spectra in fully developed turbulence, Applied Scientific Research, Volume 51, 99-103, 1993.

[8] Arya, S. P., "Atmospheric boundary layers over homogeneous terrain", Engineering Meteorology, Ed. by E. J. Plate, Elsevier Scientific Publishing Company, Amsterdam, 1982: 233-266.

[9] Cook, N.J., "A Boundary Layer Wind Tunnel for Building Aerodynamics", Journal of Industrial Aerodynamics, 1975, 1: 3-12.

[10] Sykes, D.M., "A New Wind Tunnel for Industrial Aerodynamics", Journal of Industrial Aerodynamics 1977, 2: 65-78.

[11] Greenway, M., Wood, C., "The Oxford University 4 m × 2 m Industrial Aerodynamics Wind Tunnel" Journal of Industrial Aerodynamics 1979, 4, 43-70.

[12] Blessmann, J., "The Boundary Layer TV-2 Wind Tunnel of the UFGRS", Journal of Wind Engineering and Industrial Aerodynamics, 1982, 10: 231-248.

[13] Hansen, S., Sorensen, E., "A New Boundary Layer Wind Tunnel at the Danish Maritime Institute", Journal of Wind Engineering and Industrial Aerodynamics 1985, 18: 213-224.

[14] Wittwer, A. R., Loredo-Souza, A. M., Schettini, E. B. C., Laboratory evaluation of the urban effects on the dispersion process using a small-scale model. In: 13th International Conference on Wind Engineering, Amsterdam. Proceedings of the ICWE13, 2011.

[15] Loredo Souza, A. M., "The behaviour of transmission lines under high winds", Thesis – Doctor of Philosophy, The University of Western Ontario, London, Ontario, 1996.

[16] Counihan, J., "An Improved Method of Simulating an Atmospheric Boundary Layer in a Wind Tunnel", Atmospheric Enviroment 1969, 3: 197-214.

[17] Standen, N.M., "A Spire Array for Generating Thick Turbulent Shear Layers for Natural Wind Simulation in Wind Tunnels", National Research Council of Canada, NAE, Report LTR-LA-94, 1972.

[18] A. R. Wittwer, M. E. De Bortoli, M. B. Natalini, "The importance of velocity fluctuations analysis at the atmospheric boundary layer simulation in a wind tunnel", 2nd East European Conference on Wind Engineering, Proceedings, Vol. 2, pp. 385, Academy of Sciences of the Czech Republic, Institute of Theoretical and Applied Mechanics, Czech Republic, Prague, 1998.

[19] Wittwer A. R., Möller S. V., "Characteristics of the low speed wind tunnel of the UNNE", Journal of Wind Engineering & Industrial Aerodynamics, 2000, 84: 307-320.

[20] J. Marighetti, A. Wittwer, M. De Bortoli, B. Natalini, M. Paluch, M. B. Natalini, "Fluctuating and mean pressures measurements in a wind tunnel over a stadium covering", Journal of Wind Engineering & Industrial Aerodynamics, 2000, 84: 321-328.

[21] Centro de Investigación de los Reglamentos Nacionales de Seguridad para las Obras Civiles, Reglamento CIRSOC 102, "Acción del Viento sobre las Construcciones", IN-TI, Argentina, 1982.

[22] Liu, G., Xuan, J., Park, S., "A new method to calculate wind profile parameters of the wind tunnel boundary layer", Journal of Wind Engineering and Industrial Aerodynamics 2003, 91: 1155-1162.

[23] Robins, A., Castro, I., Hayden, P., Steggel, N., Contini, D., Heist, D., "A wind tunnel study of dense gas dispersion in a neutral boundary layer over a rough surface", Atmospheric environment 2001, 35: 2243-2252.

[24] Cook, N. J., "The designer's guide to wind loading of building structures", BRE, Building Research Establishment, London, UK, 1990.

[25] Press, W.H., Flannery, B.P., Teukolsky, S.A., Vetterling, W.T., "Numerical Recipes: The Art of Scientific Computing", Cambridge University Press, New York, 1990.

[26] Acevedo, O.C., Moraes, O.L.L., Degrazia, G.A., Medeiros, L.E., "Intermittency and the exchange of scalars in the nocturnal surface layer", Boundary-layer meteorology, 119: 41-55, 2006.

[27] Wittwer A. R., Welter G. S., Degrazia G. A., "Características espectrales de la turbulencia en vientos de capa superficial", Proceedings de 1er. Congreso Latinoamericano de Ingeniería del Viento, Montevideo, Uruguay, 4 - 6 nov. 2008.

[28] Wittwer A. R., Welter G. S., Degrazia G. A., Loredo-Souza A. M., Acevedo O. C., Schettini E. B. C., Moraes O. L. L., "Espectros de turbulência medidos na camada atmosférica superficial e em um túnel de vento de camada limite.", Ciência & Natura, Revista do Centro de Ciências Naturais e Exatas, UFSM, Brasil, V. Esp. 2007: 137-141.

[29] Welter, G. S., Wittwer, A. R., Degrazia, G.A., Acevedo, O.C., Moraes, O.L.L., Anfossi, D., "Measurements of the Kolmogorov constant from laboratory and geophysical wind data", Physica A: Statistical Mechanics and its Applications, 388 : 3745-3751, 2009.

[30] Degrazia G. A., Welter G. S., Wittwer A. R., Carvalho J., Roberti D. R., Acevedo O. C., Moraes O.L.L., Velho H.F.C., "Estimation of the Lagrangian Kolmogorov constant from Eulerian measurements for distinct Reynolds number with application to pollution dispersion model", Atmospheric Environment 42, pp. 2415–2423, 2008.

[31] Degrazia, G., Anfossi, D., Carvalho, J., Mangia, C., Tirabassi, T. & Campos Velho, H. Turbulence parameterisation for PBL dispersion models in all stability conditions, Atmospheric environment 34(21): 3575–3583, 2000.

[32] Kolmogorov, A. N. (1941a). Energy dissipation in locally isotropic turbulence, Dokl. Akad. Nauk SSSR, Vol. 32, pp. 19–21, 1941.

[33] Kolmogorov, A. N. (1941b). The Local Structure of Turbulence in Incompressible Viscous Fluid for Very Large Reynolds' Numbers, Dokl. Akad. Nauk SSSR, Vol. 30, pp. 301–305, 1941.

[34] Monin A., Yaglom A., Statistical fluid mechanics: Vol. 2. [S.l.]: MIT Press, 1975.

[35] Falkovich, G., Sreenivasan, K. R. Lessons from Hydrodynamic Turbulence, Phys. Today 59, 43 (2006), DOI:10.1063/1.2207037

[36] Frisch U. Turbulence: The Legacy of AN Kolmogorov. [S.l.]: Cambridge University Press, 1995.